

A continuum traffic flow model with the consideration of coupling effect for two-lane freeways

Di-Hua Sun · Guang-Han Peng · Li-Ping Fu · Heng-Pan He

Received: 5 December 2008 / Revised: 22 April 2010 / Accepted: 6 May 2010
©The Chinese Society of Theoretical and Applied Mechanics and Springer-Verlag Berlin Heidelberg 2011

Abstract A new higher-order continuum model is proposed by considering the coupling and lane changing effects of the vehicles on two adjacent lanes. A stability analysis of the proposed model provides the conditions that ensure its linear stability. Issues related to lane changing, shock waves and rarefaction waves, local clustering and phase transition are also investigated with numerical experiments. The simulation results show that the proposed model is capable of providing explanations to some particular traffic phenomena commonly observable in real traffic flows.

Keywords Two-lane traffic · Two delay time scales model · Numerical simulation · Coupling effect · Phase transition

The project was supported by the National High Technology Research and Development Program of China (863) (511-0910-1031) and the National “10th Five-Year” Science and Technique Important Program of China (2002BA404A07).

D.-H. Sun · G.-H. Peng (✉)
College of Automation, Chongqing University,
400030 Chongqing, China
e-mail: pengguanghan@yahoo.com.cn

L.-P. Fu
Department of Civil & Environmental Engineering,
University of Waterloo, Waterloo, Ontario N2L 3G1, Canada

H.-P. He
College of Automation, Chongqing University,
400030 Chongqing, China

1 Introduction

LWR theory is the earliest and most fundamental first-order continuum traffic model proposed by Lighthill and Whitham [1] and Richards [2] independently. According to this theory, traffic flows on a long homogeneous freeway are governed by the following conservation equation

$$\frac{\partial k}{\partial t} + \frac{\partial q}{\partial x} = s(x, t), \quad (1)$$

where k is traffic density, q is traffic flow rate, x is space, t is time and $s(x, t)$ is flow generation rate. When there is no on-off ramp, $s(x, t) = 0$; otherwise, $s(x, t) \neq 0$. The equivalent flow-density relationship between flow rate q and density k is

$$q = ku. \quad (2)$$

For the speed u , as in LWR, the existence of an equilibrium speed-density relationship is assumed

$$u = u_e(k). \quad (3)$$

According to the above three equations, analytical solutions can be obtained. Some traffic flow problems, such as shock waves and traffic jams, can be addressed from these solutions.

However, the LWR model cannot be used to describe correctly the traffic flows in nonequilibrium states since the equilibrium relationship between speed and density is always assumed in the equilibrium speed-density equation (3). Many scholars have proposed high-order continuum traffic flow models that incorporate a dynamics equation or momentum equation to represent general car-following behavior [3–11]. This momentum equation takes the acceler-

ation and inertia of driving into account. Hence, the high-order models make up for some deficiencies in the simple continuum models and improve their ability to reproduce complex traffic behavior.

However, the existing high-order models have a fundamental flaw that one of the characteristic speeds resulting from the momentum and conservation equations is larger than the macroscopic flow speed. This implies that vehicles would affect the vehicles in front of them [12]. This evidently violates the anisotropy of traffic flow and does not accord with the real traffic.

On the basis of their full velocity difference (FVD) car-following model [13], Jiang et al. [12] proposed a new dynamic equation in which the density gradient term is replaced by a speed gradient term. Recently, Jiang and Wu [14] further analyzed the structural properties of the solutions of the speed gradient traffic flow model. The solutions showed that the model's characteristic speeds are not larger than the macroscopic flow speed, hence vehicles respond only to their frontal stimulus. But the propagation speed of disturbance c_0 in this model is a constant, independent of the density. In fact, the propagation speed of disturbance in a Payne-Whitham-like model should depend on the density [15,16]. Concerning the relationship between disturbance propagation speed and density, with two delay time scales taken into account, Xue and Dai [17] improved the model by treating c_0 as a function of the density, with which the undesirable "wrong-way travel" phenomenon and gas-like behavior are eliminated and the formation and diffusion of traffic shock can be better simulated.

In the above models, the following car is not allowed to overtake the leading car. Hence, these models are applicable only to the traffic flow on freeways with single lane. Daganzo [18] developed a continuum theory of traffic dynamics for freeways with two lanes allocated for two sorts of vehicles (lane 1 for faster vehicles and lane 2 for slower vehicles). The theory defines the conservation equation as

$$\frac{\partial P}{\partial t} + \frac{\partial Q}{\partial x} = S, \quad (4)$$

where $P = (k_1, k_2)^T$, $Q = [q_1(k_1, k_2), q_2(k_1, k_2)]^T$, $(s_{21} - s_{12}, s_{12} - s_{21})^T$, k_m and q_m represent the traffic density and the flow rate on lane m ($m = 1, 2$), respectively, s_{mn} represents lane changing rate from lane m to lane n . Daganzo first studied the possible relationships between the velocities and the densities based on the density ratio of the two lanes, then formulated the traffic flow models for each of totally four $k_1 - k_2$ regions. To carry out analyses graphically, Daganzo adopted simple continuum model only; hence his approach cannot be used to describe the non-equilibrium traffic flow dynamics. Wu [19] proposed a multi-lane traffic model, considering the specific traffic conditions in Chinese cities (e.g., untidy flows and lower speeds on roads), but Wu's model tends to equalize all lanes' densities through averaging them. This conflicts with the real traffic since the density on the lane allocated for faster vehicles is generally less than that on the lane al-

located for slower vehicles. Tang and Huang [20,21] lately developed a continuum model for freeways with two lanes which integrates the momentum equation proposed by Jiang et al. [12] to the Daganzo's modeling framework for multi-lane traffic flow [18]. However, this model allows only the faster vehicles to change lanes. Recently, Huang and Tang et al. [22] further extended the work of Tang and Huang [20,21] by allowing that vehicles on both lanes to change their lanes according to the traffic condition on the spot and in real time, which contains the speed gradient-based momentum equations derived from a car-following theory suited to two-lane traffic flow. Tang and Jiang et al. [23] also extended the speed gradient model to traffic flow on two-lane freeways. But the coupling effect of the interactions between vehicles on two lanes has not been taken into account in these models.

In this paper, we extend the two delay time scales model proposed by Xue et al. [17] to describe asymmetric two-lane traffic with the consideration of coupling effect, allowing that vehicles on both lanes to change their lanes according to the traffic condition on the spot and in real time. We also investigate lane changing rate resulting in the shock waves and rarefaction waves and the local cluster wave effect in two-lane freeways.

The paper is organized as follows. In Sect. 2, we establish a continuum model with anisotropy by introducing the drivers' reaction time t_r and the vehicle relaxation time T into the forward anticipation speed with the consideration of coupling effect on both lanes; thus the propagation speed of a small disturbance is related to the density. In Sect. 3, we analyze the linear stability of the new model and give necessary and sufficient conditions for ensuring the stability. Numerical results are presented in Sect. 4 to validate the theoretical analysis, and some nonequilibrium phenomena are investigated, such as small disturbance instability, shock waves and rarefaction waves, local cluster waves and phase transition. Section 5 concludes the paper with a summary of major findings and directions for future research.

2 Modeling and analysis

The two delay time scale model proposed by Xue is based on the assumption of forward anticipation [17], in which the stream speed u in the relaxation time T just reaches the anticipated value u_e corresponding to the density in time $t + t_r$ at location $x + ut_r$, where t_r is driver reaction time. The speed-density relationship can be expressed as follows

$$u(x + uT, t + T) = u_e(k(x + ut_r, t + t_r)). \quad (5)$$

Using the Taylor series expansion of Eq. (5), applying Eq. (1) and referring to Ref. [17], we get

$$\begin{aligned} \frac{\partial u}{\partial t} + (u - c(k)) \frac{\partial u}{\partial x} &= \frac{u_e(k) - u}{T}, \\ c(k) &= -k \frac{t_r}{T} \frac{du_e}{dk} \geq 0, \\ T &= T_0 [1 + E / (1 + (k/k_M)^\theta)], \end{aligned} \quad (6)$$

where $c(k)$ is the “sonic speed” in traffic flow, at which small disturbances propagate relative to a moving traffic stream. The relaxation time T is a nonlinear function of the density k . And k_M is the critical density, T_0 is the constant reaction time, θ is a parameter ($\theta > 0$), and E is a constant ($E > 0$) that denotes the difference in reaction times between congested and uncongested traffic situations. As $k \rightarrow 0$, $T \rightarrow (E+1)T_0$; when $k > k_M$, $T > T_0$. This means that at high density levels the relaxation time is smaller, and at low density levels the relaxation time is larger.

On two-lane freeways, the lane changing behaviour will occur. To model this effect, the interactions between vehicles on two lanes, i.e. the coupling effect between two lanes, must be taken into account to describe the flow rate changing from the other lane. So a coupling effect term is added to Eq. (5) to describe the flow rate changing to the other lane.

$$u_m(x + u_m T_m, t + T_m) = u_{em}[k_m(x + u_m t_{vm}, t + t_{vm}), \beta_{nm} k_n],$$

$$m, n = 1, 2, \quad \text{and} \quad m \neq n. \quad (7)$$

Equation (7) means that the stream speed u_m in the relaxation time T_m just reaches the anticipated value u_{em} (u_{em} is functions of k_1 and k_2) corresponding to the density in time $t + t_{vm}$ at the location $x + ut_{vm}$ on lane m , where t_{vm} is driver reaction time on lane m . And here β_{nm} is coupling coefficient from lane n to lane m . On the basis of principle of coupling interaction, we consider $\beta_{nm} = \beta_{mn} = \beta$. Using the Taylor series expansion of Eq. (7) and neglecting higher-order terms, we get

$$u_m(x, T_m) + \frac{\partial u_m}{\partial t} T_m + u_m T_m \frac{\partial u_m}{\partial x} + O(T_m^2) = u_{em}(k_m, \beta k_n)$$

$$+ \frac{\partial u_{em}}{\partial k_m} \times \left(t_{vm} \frac{\partial k_m}{\partial t} + u_m t_{vm} \frac{\partial k_m}{\partial x} \right) + O(t_{vm}^2). \quad (8)$$

Equation (8) can be rearranged as

$$\frac{\partial u_m}{\partial t} + u_m \frac{\partial u_m}{\partial x} = \frac{u_{em}(k_m, \beta k_n) - u_m}{T_m}$$

$$+ \frac{t_{vm}}{T_m} \frac{\partial u_{em}}{\partial k_m} \times \left(\frac{\partial k_m}{\partial t} + u_m \frac{\partial k_m}{\partial x} \right). \quad (9)$$

Applying Eq. (4), we have

$$\frac{\partial u_m}{\partial t} + (u_m - c_{m0}) \frac{\partial u_m}{\partial x} = \frac{u_{em}(k_m, \beta k_n) - u_m}{T_m}$$

$$+ \gamma_m s_{nm} - \gamma_m s_{mn}, \quad (10)$$

$$c_{m0} = -k_m \frac{t_{vm}}{T_m} \frac{\partial u_{em}(k_m, \beta k_n)}{\partial k_m} \geq 0,$$

$$\gamma_m = \frac{t_{vm}}{T_m} \frac{\partial u_{em}(k_m, \beta k_n)}{\partial k_m}.$$

The dynamics model for two-lane traffic consists of the following equations

$$\frac{\partial k_m}{\partial t} + \frac{\partial q_m}{\partial x} = s_{nm}(x, t) - s_{mn}(x, t), \quad (11)$$

$$\frac{\partial u_m}{\partial t} + (u_m - c_{m0}) \frac{\partial u_m}{\partial x} = \frac{u_{em}(k_m, \beta k_n) - u_m}{T_m}$$

$$+ \gamma_m s_{nm} - \gamma_m s_{mn}$$

$$m, n = 1, 2, \quad \text{and} \quad m \neq n, \quad (12)$$

where $c_{m0} = -k_m \frac{t_{vm}}{T_m} \frac{\partial u_{em}(k_m, \beta k_n)}{\partial k_m} \geq 0$ represents the propagation speed of the disturbance on lane m . Note that the model given by Eqs. (11) and (12) for a specific lane is formally the same as the continuum model proposed by Xue [17] (when $\beta = 0$ and $S = 0$ on a single lane). However, attention should be paid to such a difference that all the velocities in Eqs. (11) and (12) are functions of k_1 and k_2 . According to Liu's idea [24] and Tang's method [23], we suppose the analogy terms of lane changing rate have the form as follows

$$s_{12} = a Q_{e1} k_1 (1 - (k_2/k_{2jam})^\sigma), \quad (13)$$

$$s_{21} = a(1 + b(Q_{e1} - Q_{e2})) \times Q_{e2} k_2 (1 - (k_1/k_{1jam})^\phi), \quad (14)$$

where Q_{ei} is the equilibrium flow ($Q_{ei} = ku_{ei}(k)$) and σ, ϕ are the parameters that reflect the intensity of the lane-change effect from one lane to another, $0 \leq \sigma, \phi \leq 1$, and depend on the condition of road. The special case of $Q_{e1} = Q_{e2}$ corresponds to symmetric lane changing rules, while $Q_{e1} \neq Q_{e2}$ corresponds to asymmetric lane changing rules; a and b are constant parameters, k_{ijam} is the jam density of lane i .

In real traffic, the lane changing rate, say from lane 1 to 2, should be zero when either $k_2 = k_{2jam}$ (lane 2 is in complete jam) or $k_1 = 0$ (there is no vehicle on lane 1). Furthermore, it obviously depends on the equilibrium speed density relationship on the present lane and on the coupling density of the other lane. These properties are fulfilled in Eqs. (13) and (14).

We rewrite system (11) and (12) as follows

$$\frac{\partial \mathbf{V}}{\partial t} + \mathbf{A} \frac{\partial \mathbf{V}}{\partial x} = \mathbf{E}, \quad (15)$$

where

$$\mathbf{V} = \begin{Bmatrix} k_1 \\ u_1 \\ k_2 \\ u_2 \end{Bmatrix},$$

$$\mathbf{A} = \begin{bmatrix} u_1 & k_1 & 0 & 0 \\ 0 & u_1 - c_{10} & 0 & 0 \\ 0 & 0 & u_2 & k_2 \\ 0 & 0 & 0 & u_2 - c_{20} \end{bmatrix}, \quad (16)$$

$$\mathbf{E} = \begin{bmatrix} s_{21} - s_{12} \\ (u_{e1} - u_1)/T_1 + \gamma_1 s_{21} - \gamma_1 s_{12} \\ s_{12} - s_{21} \\ (u_{e2} - u_2)/T_2 + \gamma_2 s_{12} - \gamma_2 s_{21} \end{bmatrix}.$$

Comparing our new model with other continuum models presented by Daganzo [18], we can see that the new model includes two new motion equations, in which the speed gradient term replaces the density gradient term as the anti-

pation term with $c_{i0} = c(k_i)$. This replacement in the new model solves the characteristic speed problem that exists in the previous high-order models and therefore enables the new model to satisfy the anisotropic property of traffic flows. Next we apply matrixes to analyze character speeds of the system (15). The eigenvalues, λ , of matrix A are found by setting

$$\det(A - \lambda I) = 0, \quad (17)$$

where I is identity matrix. From Eq. (17), we have

$$\lambda_{11} = u_1, \quad \lambda_{12} = u_1 - c_{10},$$

$$\lambda_{21} = u_2, \quad \lambda_{22} = u_2 - c_{20}.$$

From the above-mentioned, $c_{i0} \geq 0$ ($i = 1, 2$), which means that the character speeds of each subsystem are not larger than their macroscopic flow speeds, which shows that on each lane the rear disturbances cannot propagate forward. However, it does not guarantee that in a system consisting of two lanes the rear disturbance will not affect the driving behavior of the leading vehicle because lane changing is allowed in these two-lane traffic system.

3 Linear stability condition

According to the method introduced by Huang et al. [22] and Tang et al. [23], the steady state solutions of the extended two delay time scales model can be obtained by setting the derivative terms in Eqs. (11) and (12) to zero. It means here $s_{nm} - s_{mm} = 0$ ($m, n = 1, 2$). For lane m ($m = 1, 2$), let k_m^* and u_m^* be the steady-state solutions of the model (11)–(12), $k_m = k_m^* + \xi_m$ and $u_m = u_m^* + \varepsilon_m$ be the perturbed solutions, where $\xi_m = \xi_m(x, t)$ and $\varepsilon_m = \varepsilon_m(x, t)$ represent small smooth perturbations to the steady-state solutions. Substituting $k_m = k_m^* + \xi_m$ and $u_m = u_m^* + \varepsilon_m$ into Eqs. (11) and (12), taking the Taylor series expansions at the point (k_m^*, u_m^*) and neglecting the higher order terms of ξ_m and ε_m , we obtain the following equations

$$\frac{\partial \xi_m}{\partial t} + u_m^* \frac{\partial \xi_m}{\partial x} + k_m^* \frac{\partial \varepsilon_m}{\partial x} = 0, \quad m = 1, 2, \quad (18)$$

$$\frac{\partial \varepsilon_1}{\partial t} + (u_1^* - c_{10}) \frac{\partial \varepsilon_1}{\partial x} = \frac{a\xi_1 + b\xi_2 - \varepsilon_1}{T_1}, \quad (19)$$

$$\frac{\partial \varepsilon_2}{\partial t} + (u_2^* - c_{20}) \frac{\partial \varepsilon_2}{\partial x} = \frac{c\xi_1 + d\xi_2 - \varepsilon_2}{T_2}, \quad (20)$$

where $a = \partial u_{e1}(k_1^*, \beta k_2^*) / \partial k_1$, $b = \partial u_{e1}(k_1^*, \beta k_2^*) / \partial k_2$, $c = \partial u_{2e}(\beta k_1^*, k_2^*) / \partial k_1$, $d = \partial u_{2e}(\beta k_1^*, k_2^*) / \partial k_2$. Eliminating ε_1 and ε_2 in Eqs. (18)–(20), we obtain

$$(\partial_t + c_1 \partial_x) \xi_1 = -T_1 [(\partial_t + c_{11} \partial_x)(\partial_t + c_{12} \partial_x)] \xi_1, \quad (21)$$

$$(\partial_t + c_2 \partial_x) \xi_2 = -T_2 [(\partial_t + c_{21} \partial_x)(\partial_t + c_{22} \partial_x)] \xi_2, \quad (22)$$

where $c_1 = u_1^* + k_1^*(ad - bc)/d$, $c_2 = u_2^* + k_2^*(ad - bc)/a$, $c_{11} = u_1^* - c_{10}$, $c_{12} = u_1^*$, $c_{21} = u_2^* - c_{20}$, $c_{22} = u_2^*$.

According to the traditional way of linear stability analysis, and substituting $\xi_i(x, t) = \xi_{i0} \exp i(\gamma x - wt)$, $i = 1, 2$ into Eqs. (21) and (22), we can show that

$$(-iw + ic_{11}\gamma)\xi_1 = -T_1 [(-iw + c_{11}i\gamma)(-iw + c_{12}i\gamma)]\xi_1, \quad (23)$$

$$(-iw + ic_{21}\gamma)\xi_2 = -T_2 [(-iw + c_{21}i\gamma)(-iw + c_{22}i\gamma)]\xi_2. \quad (24)$$

Because ξ_i is non-trivial solution of Eqs. (23) and (24), we must have

$$-T(w - c_{11}\gamma)(w - c_{12}\gamma) + i(w - c_{11}\gamma) = 0, \quad (25)$$

$$-T(w - c_{21}\gamma)(w - c_{22}\gamma) + i(w - c_{21}\gamma) = 0. \quad (26)$$

It is obvious that the solution is stable if and only if the imaginary part of both roots w of Eqs. (25) and (26) are non-positive. For such equations as Eqs. (25) and (26), Whitham [25] and Zhang [26] have already verified that the requirement for this is

$$c_{11} \leq c_1 \leq c_{12}, \quad (27)$$

$$c_{21} \leq c_2 \leq c_{22}. \quad (28)$$

Inequalities (27) and (28) are the criteria of stability. When one of the conditions (27) and (28) is violated, traffic instability will occur. Also inequalities (27) and (28) shows that one lane's stability is affected by its lateral lane's traffic density. Equations (21) and (22) show that linear wave is second-order wave. The second-order wave propagation speed is very similar to the characteristic speed. But the steady-state solutions u_i^* replace flow u_i for linear stability analysis. And first-order wave of both lanes propagates at the same wave speed c_1 and c_2 . However, higher-order wave propagates at different speeds, which depends on characteristic speeds. Second-order wave speeds, c_{11} and c_{12} , c_{21} and c_{22} , determine the fastest and slowest propagation speed of perturbation information for second order equation of two lane system. However, the propagation speed of first-order wave c_i is the propagation speed of main perturbation information. Thus, when the inequality $c_{11} \leq c_1 \leq c_{12}$ and $c_{21} \leq c_2 \leq c_{22}$, both are satisfied at the same time, the propagating perturbations do not conflict with each other, which assures the stability of the system. When $c_i \geq c_{i2}$ or $c_i \leq c_{i1}$, the propagation speed of main perturbation information is greater than the highest speed of information propagation or less than the lowest speed of information propagation, and the propagating perturbations will conflict with each other, which results in inextricable competition between first- and second- order wave. Only the inextricable competition leads to instability of the system.

4 Numerical simulation

In this section, using the finite difference method, we numerically solve the model to demonstrate the model's ability of capturing complex traffic phenomena. Let index j represent the time interval and index i the road section, then the dif-

ference equations corresponding to Eqs. (11) and (12) are as follows

$$k_{m(i)}^{(j+1)} = k_{m(i)}^{(j)} + \frac{\Delta t}{\Delta x} k_{m(i)}^{(j)} (u_{m(i)}^{(j)} - u_{m(i+1)}^{(j)}) + \frac{\Delta t}{\Delta x} u_{m(i)}^{(j)} (k_{m(i-1)}^{(j)} - k_{m(i)}^{(j)}) + \Delta t s_{nm(i)}^{(j)} - \Delta t s_{mn(i)}^{(j)}, \quad m, n = 1, 2. \quad (29)$$

(1) When traffic is heavy, $u_{m(i)}^{(j)} < c_{m0}$,

$$u_{m(i)}^{(j+1)} = u_{m(i)}^{(j)} + \frac{\Delta t}{\Delta x} (c_{m0} - u_{m(i)}^{(j)}) (u_{m(i+1)}^{(j)} - u_{m(i)}^{(j)}) + \frac{\Delta t}{T_1} (u_{em} - u_{m(i)}^{(j)}) + \gamma_m \Delta t s_{nm(i)}^{(j)} - \gamma_m \Delta t s_{mn(i)}^{(j)}, \quad m, n = 1, 2 \quad (30)$$

(2) When traffic is light, $u_{m(i)}^{(j)} \geq c_{m0}$,

$$u_{m(i)}^{(j+1)} = u_{m(i)}^{(j)} + \frac{\Delta t}{\Delta x} (c_{m0} - u_{m(i)}^{(j)}) (u_{m(i)}^{(j)} - u_{m(i-1)}^{(j)}) + \frac{\Delta t}{T_2} (u_{em} - u_{m(i)}^{(j)}) + \gamma_m \Delta t s_{nm(i)}^{(j)} - \gamma_m \Delta t s_{mn(i)}^{(j)}, \quad m, n = 1, 2 \quad (31)$$

4.1 Shock waves and rarefaction waves

In order to investigate congestion and dissipation of the traffic flow, we use two Riemann initial conditions [17,21].

$$(1) \begin{cases} k_{1u}^1 = 0.03, \\ k_{2u}^1 = 0.04, \end{cases} \quad \begin{cases} k_{1d}^1 = 0.12, \\ k_{2d}^1 = 0.18, \end{cases} \quad (32a)$$

$$(2) \begin{cases} k_{1u}^2 = 0.12, \\ k_{2u}^2 = 0.18, \end{cases} \quad \begin{cases} k_{1d}^2 = 0.03, \\ k_{2d}^2 = 0.04, \end{cases} \quad (32b)$$

where $k_{1u}^1, k_{2u}^1, k_{1d}^1, k_{2d}^1$ and $k_{1u}^2, k_{2u}^2, k_{1d}^2, k_{2d}^2$ are the upstream and downstream densities of two lanes, respectively. Equation (32a) corresponds to the appearance of shock waves when free-flow traffic meets stopped vehicles, while Eq. (32b) corresponds to the rarefaction wave as a queue dissolves. Two initial conditions are

$$u_{1u}^{1,2} = u_{e1}(k_{1u}^{1,2}, k_{2u}^{1,2}), \quad u_{1d}^{1,2} = u_{e1}(k_{1d}^{1,2}, k_{2d}^{1,2}), \quad (33a)$$

$$u_{2u}^{1,2} = u_{e2}(k_{1u}^{1,2}, k_{2u}^{1,2}), \quad u_{2d}^{1,2} = u_{e2}(k_{1d}^{1,2}, k_{2d}^{1,2}). \quad (33b)$$

The equilibrium speed-density relationships are obtained by substituting $k_m + \beta k_n$ into the equilibrium speed-density relationship developed by Del Castillo and Benitez [27]

$$u_{e1}(k) = u_{1f} \left\{ 1 - \exp \left\{ 1 - \exp \left[\frac{c_{1jam}}{u_{1f}} \left(\frac{k_{1jam} + \beta k_{2jam}}{k_1 + \beta k_2} - 1 \right) \right] \right\} \right\}, \quad (34a)$$

$$u_{e2}(k) = u_{2f} \left\{ 1 - \exp \left\{ 1 - \exp \left[\frac{c_{2jam}}{u_{2f}} \left(\frac{\beta k_{1jam} + k_{2jam}}{\beta k_1 + k_2} - 1 \right) \right] \right\} \right\}, \quad (34b)$$

where k_{1jam}, k_{2jam} and u_{1f}, u_{2f} are the jam densities and free-flow velocities of lane 1 and lane 2, respectively. c_{1jam}, c_{2jam}

are the propagation velocities of a disturbance under the jam densities k_{1jam}, k_{2jam} , respectively.

Free boundary conditions are applied here [12,17,21], $\partial k_m / \partial x = 0, \partial u_m / \partial x = 0$. Consider a section of freeway 20 km long, divide it into 100 cells, and take the time interval as 1 s. According to real observation and parameter identification process, the values of the parameters are chosen as follows [17,21]: $u_{1f} = 40$ m/s, $t_{r1} = 1$ s, $k_{1jam} = 0.15$ veh/m, $c_{1jam} = 7$ m/s, $u_{2f} = 30$ m/s, $t_{r2} = 0.75$ s, $k_{2jam} = 0.2$ veh/m, $c_{2jam} = 6$ m/s, $a = 0.01$, $b = 5$ s, $\beta = 0.1$, $T_0 = 7$ s, $E = 0.5$, $\theta = 1.5$, $\sigma = \phi = 1$, $k_M = 0.168$ veh/m.

Note that the jam density of lane 2 is higher than that of lane 1. The computational results under two Riemann initial conditions (32a) and (32b) are shown in Fig. 1–Fig. 6.

Figures 1, 2, 4 and 5 shows that different Riemann initial conditions lead to different fronts between the congested and the free-flow traffic, which results in proper figures of traffic flow density change on both lanes with lane changing (see Figs. 3 and 6). The wave shapes of two lanes are in accordance with that of the single lane given by Xue [17] (See Figs. 1 and 2 in Refs. [17]), which indicates that our new

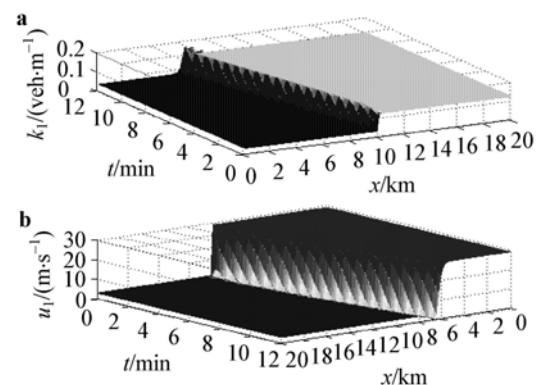


Fig. 1 Shock waves under Riemann initial conditions Eq. (32a). **a** Temporal evolution of density $k_1(x, t)$; **b** Velocity $u_1(x, t)$ on lane 1

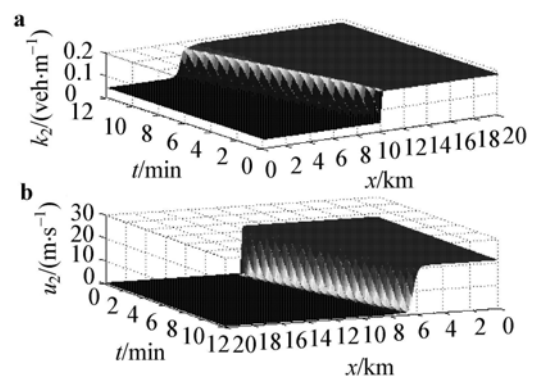


Fig. 2 Shock waves under Riemann initial conditions Eq. (32a). **a** Temporal evolution of density $k_2(x, t)$; **b** Velocity $u_2(x, t)$ on lane 2

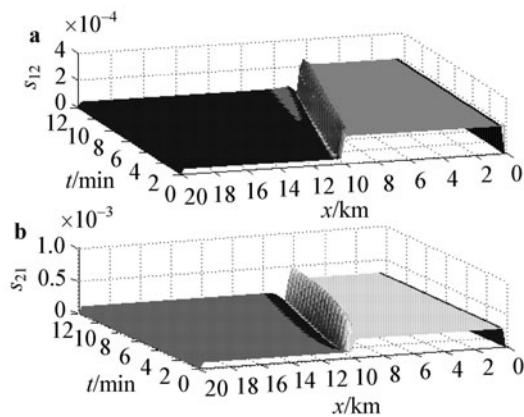


Fig. 3 Lane change rate under Riemann initial conditions Eq. (32a). **a** s_{12} is lane change rate from lane 1 to lane 2; **b** s_{21} is lane change rate from lane 2 to lane 1

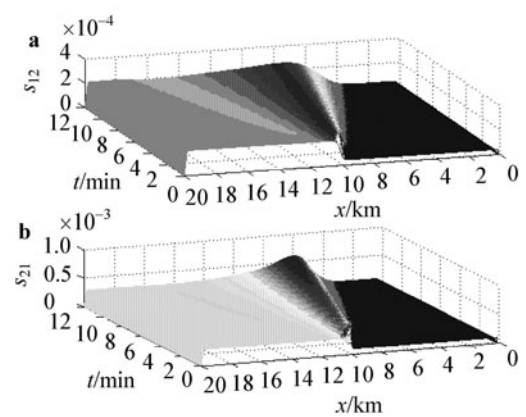


Fig. 6 Lane change rate under Riemann initial conditions Eq. (32b). **a** s_{12} is lane change rate from lane 1 to lane 2; **b** s_{21} is lane change rate from lane 2 to lane 1

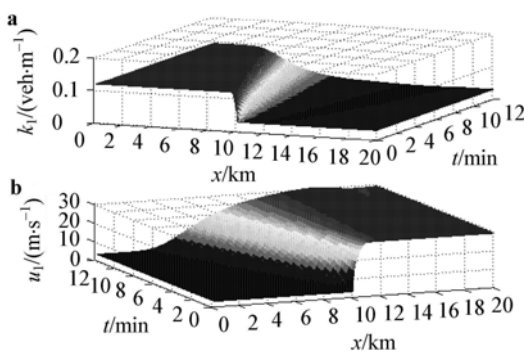


Fig. 4 Rarefaction waves under Riemann initial conditions Eq. (32b). **a** Temporal evolution of density $k_1(x, t)$; **b** Velocity $u_1(x, t)$ on lane 1

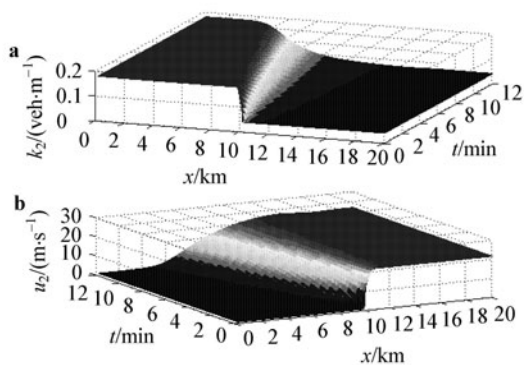


Fig. 5 Rarefaction waves under Riemann initial conditions Eq. (32b). **a** Temporal evolution of density $k_2(x, t)$; **b** Velocity $u_2(x, t)$ on lane 2

two-lane model is reasonable. Figures 1 and 2 show how the backward-moving shock wave front evolves on lane 1 and lane 2, under the condition (32a), respectively. This means that the traffic becomes more congested, which we often see in rush hours. Figures 4 and 5 show how the rarefaction wave front evolves under the condition (32b). It is a queue in the process of dissolution, which is consistent with our daily experiences in real traffic. Figures 3 and 6 show that the lane change behaviour occurs on both lanes not only at small densities but also at large densities. The results are consistent with the properties of traffic flow in Refs. [28, 29]. These effects are also consistent with the diverse nonlinear dynamics phenomena observed in realistic traffic flow.

4.2 Local cluster effect

In order to investigate the consequences caused by small localized disturbance in an initial homogenous condition, we adopt the following initial variations of the average density k_{m0} ($i = 1, 2$), which was used by Herrmann and Kerner [30]

$$k_m(x, 0) = k_{m0} + \Delta k_{m0} \left\{ \cosh^{-2} \left[\frac{160}{L} \left(x - \frac{5L}{16} \right) \right] - \frac{1}{4} \cosh^{-2} \left[\frac{40}{L} \left(x - \frac{11L}{32} \right) \right] \right\}, \quad m = 1, 2, \quad (35)$$

where $L = 32.2$ km is the length of the road section under consideration. Δk_{m0} represents perturbation. The following periodic boundary conditions are adopted

$$k_m(L, t) = k_m(0, t), \quad u_m(L, t) = u_m(0, t), \quad m = 1, 2. \quad (36)$$

The equilibrium speed-density relationships are obtained by substituting $k_m + \beta k_n$ into the equilibrium speed-density relationship developed by Kerner and Konhäuser [31]

$$u_{em} = u_{m0} \left\{ \left[1 + \exp \left[\frac{(k_m + \beta k_n)/k_{mjam} - 0.25}{0.06} \right] \right]^{-1} - 3.72 \times 10^{-6} \right\}, \quad m, n = 1, 2, \quad \text{and} \quad m \neq n, \quad (37)$$

where k_{1jam} , k_{2jam} and u_{10} , u_{20} are, the jam densities and the free-flow speed of lane 1 and lane 2, respectively. Assume the initial flows to be in local equilibrium everywhere, i.e., $u_1(x, 0) = u_{1e}(k_1(x, 0) + \beta k_2(x, 0))$, $u_2(x, 0) = u_{2e}(\beta k_1(x, 0) + k_2(x, 0))$. Other parameters are as follows [17,35]: $\beta = 0.1$, $\Delta k_{10} = 0.008$ veh/m, $\Delta k_{20} = 0.01$ veh/m, $\Delta x = 100$ m, $\Delta t = 1$ s, $u_{10} = 40$ m/s, $u_{20} = 30$ m/s, $t_{r1} = 1$, $t_{r2} = 0.75$, $k_{1jam} = 0.15$ veh/m, and $k_{2jam} = 0.2$ veh/m, $a = 0.01$, $b = 5$ s, $\beta = 0.1$, $\sigma = \phi = 1$, $T_0 = 7$ s, $E = 0.5$, $\theta = 1.5$, $k_M = 0.168$ veh/m.

Figures 7–14 show the temporal evolution of traffic with localized perturbations k_{i0} ($i = 1, 2$). The scales of space x , time t and density k_i are 100 m, 1 s and 1 veh/m, respectively. And some new results are shown as follows.

(1) Under uncongested traffic conditions as shown in Figs. 7 and 8 ($k_{10} = 0.02$; $k_{20} = 0.035$), the perturbation dissipated quickly and the traffic flow in both lanes was in a stable condition (Fig. 7). And a few vehicles changed lane on both lanes (Fig. 8). Therefore the front car can be free for speeding up, which results in the perturbation wave surface propagating ahead.

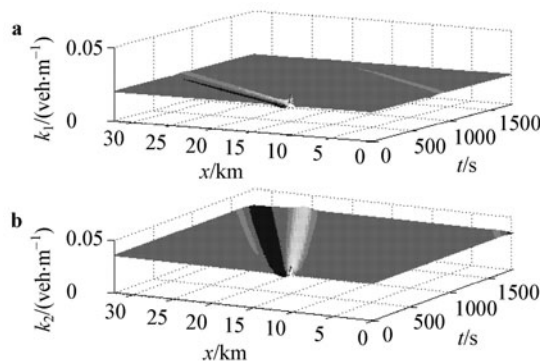


Fig. 7 Temporal evolution of density when $k_{10} = 0.02$, $k_{20} = 0.035$

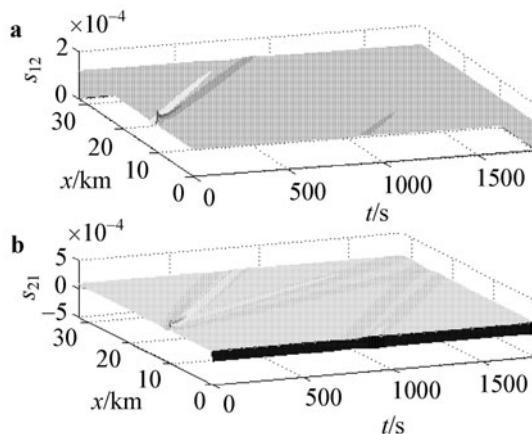


Fig. 8 $k_{10} = 0.02$, $k_{20} = 0.035$. **a** s_{12} is lane changing rate from lane 1 to lane 2; **b** s_{21} is lane changing rate from lane 2 to lane 1

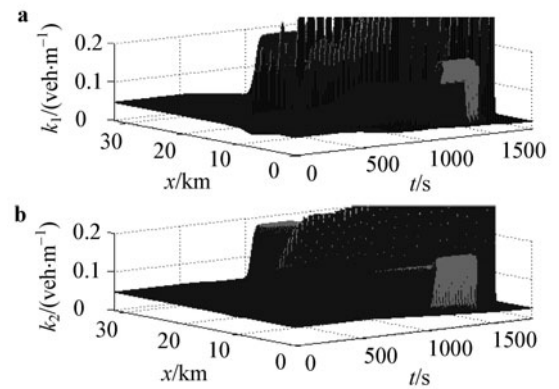


Fig. 9 Temporal evolution of density when $k_{10} = 0.047$, $k_{20} = 0.047$

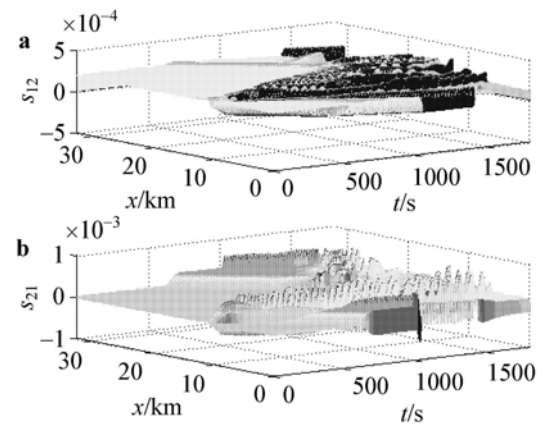


Fig. 10 $k_{10} = 0.047$, $k_{20} = 0.047$. **a** s_{12} is lane changing rate from lane 1 to lane 2; **b** s_{21} is lane changing rate from lane 2 to lane 1

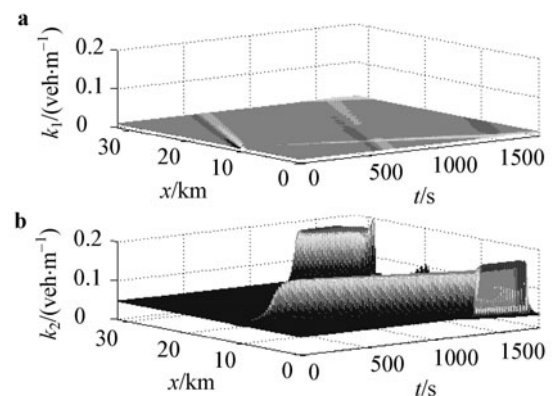


Fig. 11 Temporal evolution of density when $k_{10} = 0.01$, $k_{20} = 0.047$

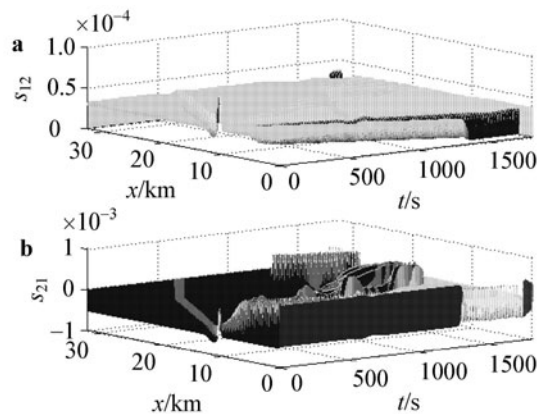


Fig. 12 $k_{10} = 0.01$, $k_{20} = 0.047$. **a** s_{12} is lane changing rate from 1 lane to 2 lane; **b** s_{21} is lane changing rate from 2 lane to 1 lane

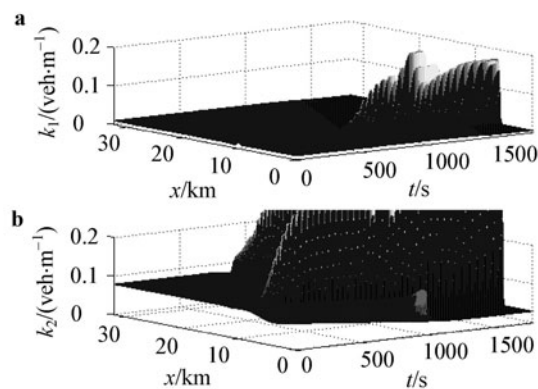


Fig. 13 Temporal evolution of density when $k_{10} = 0.01$, $k_{20} = 0.078$

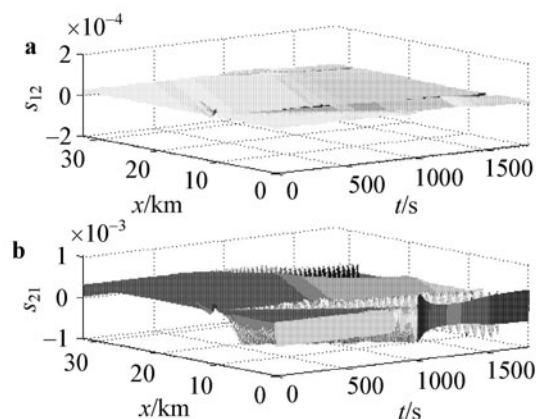


Fig. 14 $k_{10} = 0.01$, $k_{20} = 0.078$. **a** s_{12} is lane changing rate from lane 1 to lane 2; **b** s_{21} is lane changing rate from lane 2 to lane 1

(2) When the traffic density is increased to a certain level, traffic breakdown may occur if a perturbation is exerted on two lanes and some local clusters appeared, as shown in Fig. 9 and Fig. 10. A number of vehicles on both lanes made lane changing (Fig. 10). It implies that there occurs more high frequency of lane changing at large densities, which is

consistent with our daily experiences in real traffic and psychological factor of drivers.

(3) When k_{10} decreases to 0.01 while k_{20} remains unchanged, the stop-and-go traffic phenomenon still exists in lane 2 but the traffic on lane 1 is stable as seen from Fig. 11. And the traffic on lane 2 is less serious than case (2). It shows that lane 1 attracts considerable number of vehicles from lane 2 (Fig. 12) and thus alleviates the jam on lane 2.

(4) When k_{20} increases to 0.078 while k_{10} remains unchanged, as shows in Fig. 13. The stop-and-go traffic exists on both lanes but the traffic on lane 2 still experiences serious jam. This implies that the excessive lane changing from lane 2 to lane 1 (many vehicles on lane 2 shift to lane 1, then a few of them go back to lane 2 results in local jams on lane 1 (see Fig. 14).

5 Conclusions

In this paper, the two delay time scale continuum traffic model has been extended to a two-lane traffic flow. Lane changing behaviour is incorporated into the extended model by introducing a source term of lane changing rate and considering the coupling effect between two lanes in the continuity equation and two corresponding terms in the speed dynamic equations. Our model is different from previous ones in that the source term and the coupling effect are modeled separately. In this way, the lane changing rate can be investigated.

The model has anisotropy, which is confirmed by the formation and diffusion of a traffic shock wave in numerical simulations and validated by using the model. Moreover, the model has an analogy with Zhang's, Jiang and Wu's and Xue's models. In our numerical simulation of local cluster effect, our proposed model provided intuitively acceptable explanation on some common traffic behaviours. It is shown that when the density is low, perturbations can be absorbed quickly, causing only limited local effects. However, with the increase of density, the effect of perturbations also increases quickly. Our model concluded that in congested traffic a perturbation on either lane would induce a local cluster and significant lane changing activities. While these findings make intuitive sense in general, they need to be validated quantitatively using field data, which is part of our current research.

References

- 1 Lighthill, M.J., Whitham, G.B.: On kinematic waves: A theory of traffic flow on long crowded roads. *Proc. R. Soc. London-Ser. A*. **229**, 317–345 (1955)
- 2 Richards, P.I.: Shock waves on the highway. *Operations Research*. **4**, 42–51 (1956)

- 3 Payne, H.J.: Models of Freeway Traffic and Control. *Mathematical Methods of Public Systems*. **1**, 51–60 (1971)
- 4 Newell, G.: Nonlinear effects in the dynamics of car following. *Operations Research*. **9**, 209–229 (1961)
- 5 Daganzo, C.F.: Requiem for second-order fluid approximation of traffic flow. *Transportation Research-B*. **29**, 277–286 (1995)
- 6 Del Castillo, J.M., Pintado, P., Benitez, F.G.: A formulation of reaction time of traffic flow models. In: Daganzo, C.F. ed. *Transportation and Traffic Theory*. Elsevier, Amsterdam. 387–405 (1993)
- 7 Kihne, R.D.: Macroscopic freeway model for dense traffic-stopstart waves and incident detection. In: Volmuller J., Hamerslag R., eds. *Proceedings of 9th International Symposium on Transportation and Traffic Theory*. VNU Science Press, Netherland, 21–42 (1984)
- 8 Ross, P.: Traffic dynamics. *Transportation Research-B*. **22**, 421–435 1988,
- 9 Papageorgiou, M., Blosseville, J.M., Hadj-Salem H.: Macroscopic modeling of traffic flow on the Boulevard Peripherique in Paris. *Transportation Research-B*. **23**, 29–47 (1989)
- 10 Michalopoulos, R., Yi, P., Lyrintzis, A.S.: Continuum modeling of traffic dynamics for congested freeways. *Transportation Research-B*. **27**, 315–332 (1993)
- 11 Zhang, H.M.: A theory of nonequilibrium traffic flow. *Transportation Research-B*. **32**, 485–498 (1998)
- 12 Jiang, R., Wu, Q.S., Zhu, Z.J.: A new continuum model for traffic flow and numerical tests. *Transportation Research-B*. **36**, 405–419 (2002)
- 13 Jiang, R., Wu, Q.S., Zhu Z.J.: Full velocity difference model for a car-following theory. *Phys. Rev. E*. **64**, 017101 (2001)
- 14 Jiang, R., Wu, Q.S.: Analysis of the structural properties of the solutions to speed gradient traffic flow model. *Acta Mechanica Sinica*. **20**, 106–112 (2004)
- 15 Jiang, R., Wu, Q.S.: Study on propagation speed of small disturbance from a car-following approach. *Transportation Research-B*. **37**, 85–99 (2003)
- 16 Zhang, H.M.: On the consistency of a class of traffic flow models. *Transportation Research-B*. **37**, 101–105 (2003)
- 17 Xue, Y., Dai, S.Q.: Continuum traffic model with the consideration of two delay time scales. *Phys. Rev. E*. **68**, 066123 (2003)
- 18 Daganzo, C.F.: A continuum theory of traffic dynamics for freeways with special lanes. *Transportation Research-B*. **31**, 83–102 (1997)
- 19 Wu, Z.: A fluid dynamics model for low speed traffic system. *Acta Mechanica Sinica*. **26**, 149–157 (1994) (in Chinese)
- 20 Tang, T.Q., Huang, H.J.: Traffic flow model of two lanes and numerical calculation. *Chinese Science Bulletin*. **49**, 1937–1943 (2004)
- 21 Tang, T.Q., Huang, H.J.: Wave properties of a traffic flow model for freeways with two lanes. *Journal of Beijing University of Aeronautics and Astronautics*. **31**, 1121–1124 (2005)
- 22 Huang, H.J., Tang, T.Q., Gao, Z.Y.: Continuum modeling for two-lane traffic flow. *Acta Mechanica Sinica*. **22**, 131–137 (2006)
- 23 Tang, C.F., Jiang, R., Wu, Q.S.: Extended speed gradient model for traffic flow on two-lane freeways. *Chinese Physics*. **16**, 1570–1576 (2007)
- 24 Liu, G.Q.: Modelling of freeway merging and diverging flow dynamics. *Appl. Math. Model*. **20**, 459–469 (1996)
- 25 Whitham, G.B.: *Linear and nonlinear waves*. John Wiley and Sons, Inc, New York (1974)
- 26 Zhang, H.M.: Analyses of the stability and wave properties of a new continuum traffic theory. *Transportation Research-B*. **33**, 399–415 (1999)
- 27 Del Castillo, J.M., Benitez, F.G.: On functional form of the speed-density relationship—I: general theory. *Transportation Research-B*. **29**, 373–406 (1995)
- 28 Wager, P., Nagel, K., Wolf, D.E.: Realistic multi-lane traffic rules for cellular automata. *Physica A*. **234**, 687–698 (1997)
- 29 Knospe, W., Santen, L., Schadschneider, A., et al.: A realistic two-lane traffic model for highway traffic. *J. Phys. A*. **35**, 3369–3388 (2002)
- 30 Herrmann, M., Kerner, B.S.: Local cluster effect in different traffic flow models. *Physica A*. **255**:163–188 (1998)
- 31 Kerner, B.S., Konhäuser, P.: Cluster effect in initially homogeneous traffic flow. *Phys. Rev. E*. **48**, R2335–2338 (1993)